RNA (1995), *1*:1018–1028. Cambridge University Press. Printed in the USA.

The ribosomal environment of tRNA: Crosslinks to rRNA from positions 8 and 20:1 in the central fold of tRNA located at the A, P, or E site

JUTTA RINKE-APPEL, NICOLE JÜNKE, MONIKA OSSWALD, and RICHARD BRIMACOMBE
Max-Planck-Institut fuer Molekulare Genetik, AG Ribosomen, Ihnestrasse 73, D-14195 Berlin, Germany

ABSTRACT

The naturally occurring nucleotide 3-(3-amino-3-carboxy-propyl) uridine (''acp3U'') at position 20:1 of lupin tRNA^{Met} was coupled to a photoreactive diazirine derivative. Similarly, the 4-thiouridine at position 8 of *Escherichia coli* tRNA^{Phe} was modified with an aromatic azide. Each of the derivatized tRNAs was bound to *E. coli* ribosomes in the presence of suitable mRNA analogues, under conditions specific for the A, P, or E sites. After photoactivation of the diazirine or azide groups, the sites of crosslinking from the tRNAs to 16S or 23S rRNA were analyzed by our standard procedures, involving a combination of ribonuclease H digestion and primer extension analysis. The crosslinked ribosomal proteins were also identified. The results for the rRNA showed a well-defined series of crosslinks to both the 16S and 23S molecules, the most pronounced being (1) an entirely A-site-specific crosslink from tRNA position 20:1 to the loop-end region (nt 877–913) of helix 38 of the 23S RNA (a region that has not so far been associated at all with tRNA binding), and (2) a largely P-site-specific crosslink from tRNA position 8 to nt 2111–2112 of the 23S RNA (nt 2112 being a position that has previously been identified in footprinting studies as belonging to the ribosomal E site). The data are compared with results from a parallel study of crosslinks from position 47 (also in the central fold of the tRNA), as well as with previously published crosslinks from the anticodon loop (positions 32, 34, and 37) and the CCA-end region (position 76, and the aminoacyl residue).

Keywords: 3D model-building studies; modified nucleotides in tRNA; photoreactive derivatives; primer extension analysis; ribonuclease H digestion; topography of rRNA

INTRODUCTION

When two tRNA molecules are bound to the ribosome at the A and P sites, their CCA ends have to be in contact at the peptidyl transferase center on the 50S subunit to enable peptide bond formation to occur, and their anticodon loops are also close together via the interactions with adjacent codons on the mRNA in the 30S subunit. These stereochemical constraints have the effect of forcing the "elbow" or "central fold" regions of the two L-shaped tRNAs apart (e.g., Sundaralingam et al., 1975), so that—even if the angle between the planes of the molecules is made relatively small (Smith & Yarus, 1989)—there is still a substantial separation between the respective elbow regions. It follows that a precise analysis of contact or crosslink sites between the ribosome and the central fold of tRNA molecules located at the A and P (or E) sites should yield well-differentiated results that would be particularly useful for determining the topography of the ribosomal components in the 30S-50S subunit interface area. This contention is underscored by recent high-resolution electron microscopic reconstructions of *Escherichia coli* 70S ribosomes in vitreous ice (Frank et al., 1995; Stark et al., 1995), which indicate that tRNA-ribosome contacts from the central fold would be expected to occur to the "head" of the 30S subunit, to the "central protuberance" of the 50S subunit, and to the "bridge" connecting the two subunits, as well as possibly to other regions such as the "side lobe" of the 30S subunit, or the "L1 protuberance" and the "L7/12 stalk" of the 50S subunit. (See Frank et al. [1991] for a description of these terms in relation to the 70S structure.)

Previous crosslinking studies involving the central fold of the tRNA have concentrated on identifying the

Reprint requests to: Richard Brimacombe, Max-Planck-Institut fuer Molekulare Genetik, Ihnestrasse 73, D-14915 Berlin, Germany.

ribosomal proteins that are located in this neighborhood. These studies include crosslinks from azido derivatives attached to natural modified nucleotides at tRNA positions 8 (Lin et al., 1984), 47 (Ofengand et al., 1986), or 20:1 (Podkowinski & Gornicki, 1991), as well as direct UV-induced crosslinks from a number of positions in the elbow region (Abdurashidova et al., 1989, 1990). More recently, we have begun a corresponding analysis of crosslinks to the 16S and 23S ribosomal RNA molecules, using photoreactive labels attached to the same tRNA positions just mentioned, namely 8, 47, and 20:1. We had previously published the identification of a crosslink from the 3-(3-amino-3-carboxy-propyl) uridine residue ("acp^{3}U") at position 47 of *E. coli* tRNA^{Phe} to nt 2309 of the 23S RNA (Mitchell et al., 1993); this crosslink was formed from P-site-bound tRNA, and the crosslinking reagent was the *N*-hydroxysuccinimide ester of *p*-azido hippuric acid. Since then, we have analyzed a series of crosslinks to the 16S and 23S rRNA molecules from the same position of tRNA^{Phe} bound to the A, P, or E sites, using the *N*-hydroxysuccinimide ester of 4-(trifluoromethyl diazirino)-benzoic acid ("TDB;" Bochkareva et al., 1988) as the crosslinking moiety (Osswald et al., 1995). In this paper, we describe crosslinks both from the acp^{3}U residue at position 20:1 of lupin tRNA^{Met} (derivatized with TDB), and from the 4-thiouridine residue at position 8 of *E. coli* tRNA^{Phe} (derivatized by reaction with *p*-azido phenacyl bromide ["APAB;" Hixson & Hixson, 1975]). As in our experiments with tRNA^{Phe} derivatized at position 47, well-defined patterns of crosslinking were observed in each case from the three ribosomal sites (A, P, and E), involving ribosomal proteins from both subunits as well as the 16S and 23S rRNA molecules.

Together with these new data, there is now a substantial body of crosslinking information from the three principal regions of the tRNA molecule—the anticodon loop, the central fold, and the CCA end—to the 16S or 23S rRNA. Data from the anticodon loop include the classical P-site "zero-length" crosslink from position 34 to nt 1400 of the 16S RNA (Prince et al., 1982), and a crosslink from position 37 of E-site bound tRNA to a site close to the 3′-terminus of the latter (Wower et al., 1993), as well as a series of A-, P-, and E-site crosslinks from tRNA$_f^{Arg}$ derivatized at the thiocytidine residue in position 32 (Döring et al., 1994). At the CCA end, an azidoadenosine derivative at position 76 of P-site bound tRNA has been linked to nt 1945 of the 23S RNA (Wower et al., 1989), and a number of crosslinks from the immediately adjacent aminoacyl residue to 23S RNA have also been reported (Steiner et al., 1988; Mitchell et al., 1993; Stade et al., 1994). These data are summarized in the Discussion and form a basis for defining the ribosomal environment of tRNA that will have to be taken into account in our current and future rRNA model-building studies (cf. Brimacombe, 1995; Stark et al., 1995).

RESULTS

Binding derivatized tRNAs to the ribosome

The acp^{3}U residue at position 20:1 of lupin elongator tRNA^{Met} reacts specifically with *N*-hydroxysuccinimide esters (Podkowinski & Gornicki, 1991), and, in this series of experiments, we made use of the *N*-hydroxysuccinimide ester of the diazirine derivative TDB (Bochkareva et al., 1988), as described in the Materials and methods. Podkowinski and Gornicki (1991) have demonstrated that this type of derivatization at position 20:1 does not appreciably reduce the ability of the lupin tRNA^{Met} to bind to the ribosome. Our own assays (data not shown) confirmed their observation. The tRNA^{Met} was ^{32}P-labeled at its 5′ terminus. For EF-Tu-dependent binding to the ribosomal A site, the derivatized tRNA^{Met} ("TDB–tRNA^{Met}") was charged with methionine, and was then bound to *E. coli* 70S ribosomes (tight couples, or reconstituted from 30S and 50S subunits) that had been programmed with tRNA^{Arg} in the presence of an mRNA analogue (mRNA-1, see the Materials and methods) containing the coding sequence CGU AUG GAA (Arg Met Glu); derivatization of the tRNA was carried out prior to charging, so as to avoid concomitant modification of the α-amino group of the methionyl residue. For P-site binding, uncharged TDB–tRNA^{Met} was bound directly to the ribosomes in the presence of the same mRNA analogue. In the case of the E site, the ribosomes were programmed with tRNA^{Glu}, again using mRNA-1, followed by binding of uncharged TDB–tRNA^{Met}. Alternatively, the TDB–tRNA^{Met} P-site complex just mentioned was translocated to the E site by binding Glu–tRNA^{Glu} to the A site, followed by addition of EF-G and GTP. The various ribosomal complexes containing TDB–tRNA^{Met} were irradiated with UV light at 350 nm (Tate et al., 1990; Bochkariov & Kogon, 1992) to activate the diazirine reagent and generate the crosslinks.

In a previous series of experiments (Döring et al., 1994), we used a bromacetylamino diazirine derivative to specifically modify the thiocytidine residue at position 32 of tRNA$_f^{Arg}$. The tRNA$_f^{Arg}$ also contains a 4-thiouridine residue at position 8, as does *E. coli* tRNA^{Phe}, but this is not reactive to the diazirine derivative (Döring et al., 1994). Accordingly, in order to modify the 4-thiouridine at position 8 in the tRNA^{Phe}, we reverted to the use of the azido derivative APAB (Hixson & Hixson, 1975), which is known to react specifically and essentially quantitatively with the 4-thiouridine residue, without significantly affecting the ribosome-binding properties of the tRNA^{Phe} (Hsu et al., 1994). In this case, for EF-Tu-dependent binding to the A site, ^{32}P-labeled tRNA^{Phe} was first charged with phenylalanine and then modified with APAB (APAB does not react with the aminoacyl moiety [Hsu et al., 1984]). The charged APAB–tRNA^{Phe} was added to ribosomes

that had been programmed with $tRNA^{fMet}$ in the presence of an mRNA analogue containing the coding sequence AUG UUC (Met Phe; mRNA-2, see the Materials and methods). For P-site binding, uncharged $tRNA^{Phe}$ was modified with APAB, and bound directly to the ribosomes in the presence of mRNA-2. For E-site binding, mRNA-3 was used in which the AUG and UUC codons are reversed (UUC AUG), and the uncharged APAB–$tRNA^{Phe}$ was added after binding of $tRNA^{fMet}$. Although binding tRNA to a codon "upstream" of the initiator codon represents a nonphysiological situation, our previous experiments (Döring et al., 1994) have shown this to be an effective way of binding a modified tRNA to the E site. The ribosomal complexes containing APAB–$tRNA^{Phe}$ were photoactivated by irradiation at wavelengths above 280 nm, as described in the Materials and methods.

Isolating crosslinked complexes

The irradiated complexes containing either TDB–$tRNA^{Met}$ or APAB–$tRNA^{Phe}$ were applied to a series of three sucrose gradients (Stade et al., 1989), the first at high magnesium to separate the 70S ribosomal complexes from unbound tRNA and mRNA, the second at low magnesium to dissociate the 30S and 50S subunits, and the third in SDS to separate fractions, respectively, containing ribosomal proteins and 16S or 23S rRNA, carrying the crosslinked ^{32}P-labeled tRNA. In all of the complexes with the two derivatized tRNAs, crosslinking to both ribosomal subunits was observed in the second sucrose gradients, and the distribution of radioactivity between the RNA and protein fractions in the SDS gradients showed that the crosslinking was predominantly to the proteins, the reaction with the rRNA moiety being generally lower by a factor of 3–10. The overall yields of crosslinking were of the order of 3–5%, these values lying in the usual range for diazirine or azido derivatives, where the short-lived free radicals generated during the irradiation process (Brunner et al., 1980; Bochkariov & Kogon, 1992) react to a large extent with the solvent. Control experiments with nonirradiated tRNA–ribosome complexes, or complexes containing derivatized tRNA that had been irradiated prior to binding to the ribosome, showed zero levels of crosslinking.

The crosslinked proteins were identified by gel electrophoresis followed by immunological analysis (Gulle et al., 1988). However, we do not show these data here, because the results were essentially identical to those found with $tRNA^{Phe}$ derivatized at position 47 (Osswald et al., 1995). The crosslinked protein identification documented in this latter paper from the 30S subunit involved S19, together with traces of S9 and S13 at the A site, S7, S9, and S13 at the P site, and S7 at the E site. From the 50S subunit, L16 and L27 were found at the A site, L1, L5, L27, and L33 at the P site, and L1 and L33 at the E site. The only significant difference in the current series of experiments was that both P- and E-site-bound APAB–$tRNA^{Phe}$ gave strong crosslinking to protein S11 in the 30S subunit, instead of to proteins S7, S9, or S13 (data not shown). The differentiated patterns of protein crosslinking serve to indicate a corresponding specificity in the binding of the derivatized tRNAs to the A, P, or E sites.

Of more interest to us are the crosslinks to 16S or 23S rRNA. In the case of TDB–$tRNA^{Met}$, similar levels of crosslinking to rRNA were observed from the A and P sites, the level of reaction with 23S RNA being two- or threefold higher than that to 16S RNA. The amount of crosslinking to rRNA from the E site was, on the other hand, much lower, regardless of whether the E-site binding was made directly, or by translocation from the P site, as described above; here the distribution of crosslinking between the 16S and 23S molecules was roughly equal. No significant differences in crosslinking were observed between preparations made with 70S tight couples and those made with 70S ribosomes reconstituted from 30S and 50S subunits. In the case of APAB–$tRNA^{Phe}$, the crosslinking to rRNA was very low from both the A and E sites, whereas from the P site, a higher level was found, distributed roughly equally between the 16S and 23S RNA. Although the absolute levels of crosslinking tended to be somewhat variable, the patterns and specificities of the principal crosslink sites on the 16S and 23S RNA molecules were very reproducible.

Determination of crosslink sites on rRNA

In order to localize the crosslink sites on the rRNA, the 23S or 16S RNA complexes linked to ^{32}P-labeled TDB–$tRNA^{Met}$ or APAB–$tRNA^{Phe}$ were subjected to a series of digestions by ribonuclease H in the presence of oligodeoxynucleotides (10- or 17-mers) complementary to selected sequences on the rRNA molecules (Döring et al., 1994; Stade et al., 1994). After "scanning" the whole rRNA molecule in this way using pairs of oligodeoxynucleotides spanning 100–200-nt segments of the rRNA, those regions found to contain crosslinks were subjected to further digestions in the presence of different pairs of oligodeoxynucleotides so as to narrow down the position of the crosslink site as far as possible (Döring et al., 1994; Stade et al., 1994). Examples of the polyacrylamide gels used to separate the products of these digestions are illustrated in Figure 1. Next, 100–200-nt fragments of the rRNA encompassing the crosslink sites were isolated—again by ribonuclease H digestion—and the crosslink sites were identified, where possible, by primer extension analysis (Moazed et al., 1986; Döring et al., 1994); examples of these gels are given in Figure 2. The combined results of a large number of experiments are summarized in Table 1, and the locations of the various crosslink sites within ele-

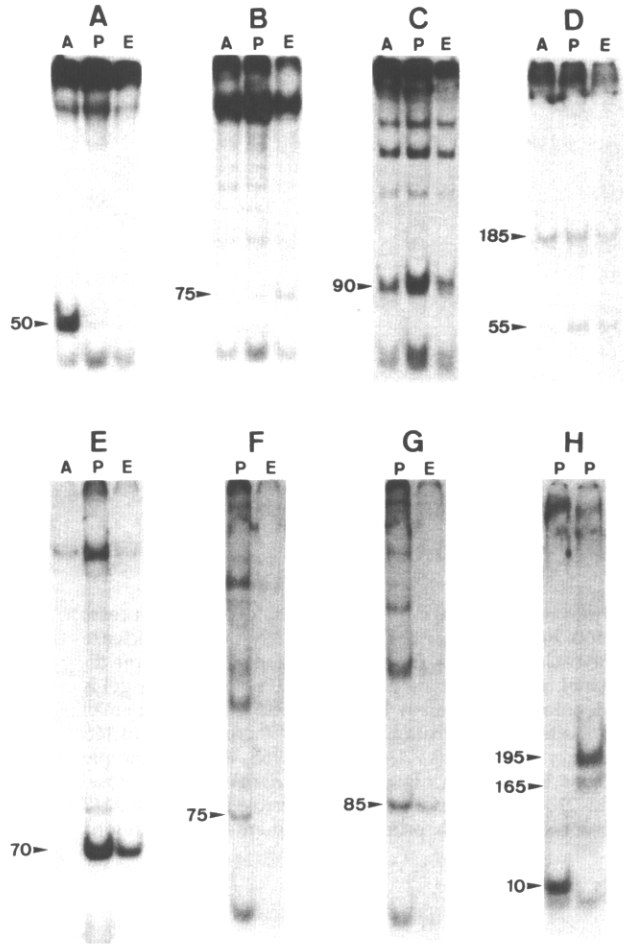

FIGURE 1. Autoradiograms of ribonuclease H digests of crosslinked A, P, or E site tRNA-16S or tRNA-23S complexes, containing ^{32}P-labeled tRNA. **A–D:** Lupin tRNA^{Met} (derivatized at position 20:1). **E–H:** *E. coli* tRNA^{Phe} (derivatized at position 8). Digestions were made in the presence of pairs of oligodeoxynucleotides centred on two 16S or 23S RNA positions, respectively, as follows. **A:** 23S positions 865 and 913, releasing a fragment of ca. 50 nt. **B:** 23S positions 2088 and 2163 (a ca. 75-nt fragment). **C:** 23S positions 2511 and 2603 (ca. 90 nt). **D:** 16S positions 1302 and 1358 (a ca. 55-nt fragment, plus a ca. 185-nt fragment from position 1358 to the 3′ terminus). **E:** 23S positions 2102 and 2170 (ca. 70 nt). **F:** 23S positions 2281 and 2358 (ca. 75 nt). **G:** 23S positions 2358 and 2442 (ca. 85 nt). **H:** 16S position 1531 (left slot; a ca. 10-nt fragment), and 16S positions 1349 and 1378 (right slot; fragments of ca. 195 and 165 nt, respectively—see text). The fast-moving band in each gel slot corresponds to free tRNA (cf. Döring et al., 1994).

TABLE 1. Summary of crosslinks to 23S and 16S RNA from position 20:1 or 8 of tRNA at the ribosomal A, P, and E sites.[a]

tRNA position	rRNA	Localization by RNAse H	Crosslink site(s) by primer extension	A	P	E
20:1	23S	877–913	–	++	–	–
		1904–1933	–	+	+	+
		2088–2114	–	–	(+)	+
		2281–2310	2309	++	++	+
		2460–2495	2476	+	++	+
		2572–2603	2574	–	++	+
		2572–2603	(2586)	+	–	–
20:1	16S	687–727	694, 711	++	++	+
		687–727	701	–	–	+
		1318–1358	(1335), 1342, (1348)	+	+	+
		1465–1500	–	+	–	–
		1500–1542	–	+	+	+
8	23S	865–913	(889)	+	–	–
		1845–1892	–	–	+	–
		2102–2163	2111, 2112	–	++	+
		2281–2358	–	–	+	–
		2398–2442	(2428)	–	+	(+)
8	16S	1317–1350	1338, 1339	–	+	–
		1531–1542	–	–	++	+

[a] The shortest RNA region encompassing each crosslink site as determined by ribonuclease H digestion (cf. Fig. 1) and the corresponding crosslinked positions as determined by primer extension analysis (cf. Fig. 2) are shown. In the primer extension column, "–" indicates that no reproducible stop signal was observed; minor stop sites, or those not always observed, are in parentheses. Distribution of the crosslinks between the A, P, and E sites is denoted by "++" (major) or "+" (minor). Here the symbol "–" means that the crosslink concerned was either absent or drastically reduced in relation to the corresponding crosslink from one of the other two tRNA sites, and in the latter case is thus regarded as a cross-contamination; "(+)" means that it was unclear whether there was a genuine contribution from the tRNA site concerned. (Note: The limits of the RNA regions defined by the ribonuclease H digestions are given in each case to the midpoint of the sequence complementary to the oligodeoxynucleotide concerned. Depending on the precise sites of ribonuclease H cleavage, these regions may of course be extended by up to two or three nucleotides in either direction).

ments of the 16S or 23S rRNA secondary structures are shown in Figures 3 and 4 (see the Discussion).

Before describing the results in detail, some comments must be made concerning the interpretation of the crosslinking data from the A, P, or E sites. As already noted above, the levels of crosslinking obtained with diazirine or azido reagents are normally very low, and, furthermore, there are considerable variations in intensity between the different individual crosslink sites on the ribosomal RNA. In this situation, the functional tests that are usually applied to determine the site-specificity of the tRNA binding to the ribosome are not appropriate for making unequivocal assignments of the corresponding site-specificity of the observed crosslinks. Thus, for example, a puromycin test might indicate that 90% of the bound tRNA is at the A site in a particular experiment, with the residual 10% being bound to the P site; if, however, this residual P-site-bound tRNA happens to be crosslinked relatively strongly to a particular position on the ribosomal RNA, then—on the basis of the puromycin result alone—that crosslink would be incorrectly assigned to the A site. The solution to this dilemma is, as we have done before (Döring et al., 1994; Osswald et al., 1995), to make parallel crosslinking analyses under A-, P-, and E-site conditions in every experiment; in the example just cited, the "residual P-site" crosslink would show up much more strongly in the P-site sample than in the

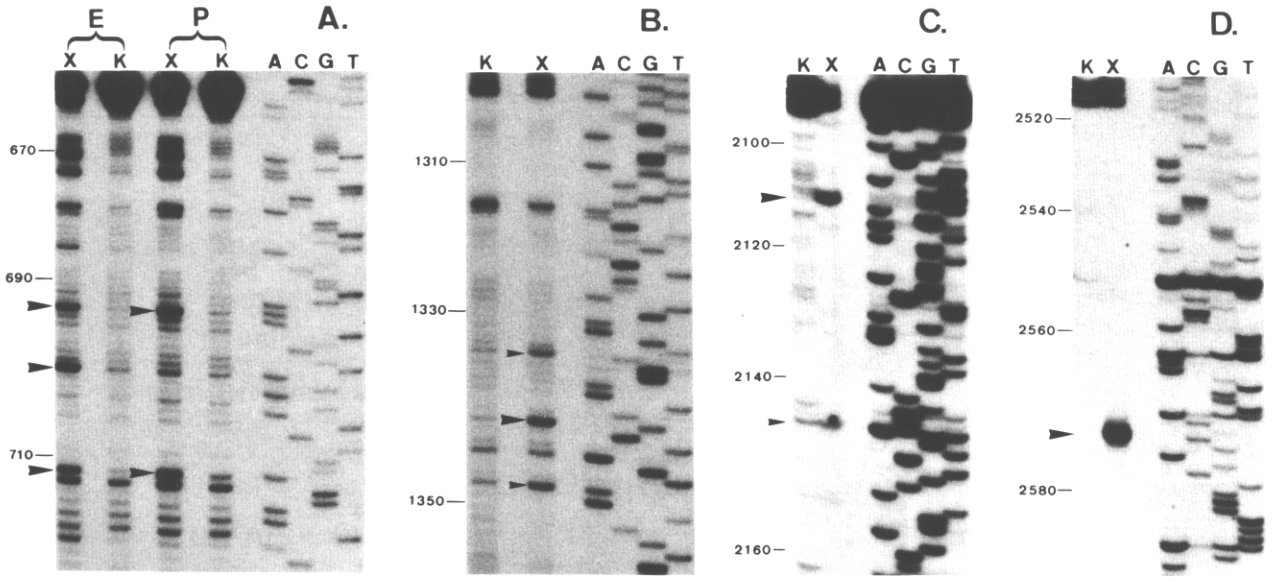

FIGURE 2. Examples of autoradiograms of primer extension analyses of individual crosslinked complexes. In each case, lane X is a crosslinked sample, isolated as a complex containing a 100–200-nt fragment of 16S or 23S RNA by ribonuclease H digestion (cf. Fig. 1). Lane K is the corresponding free (i.e., noncrosslinked) RNA fragment, isolated from the same digestion. A, C, G, and T are dideoxy sequencing lanes. In each panel, an appropriate part of the 10% sequencing gel is shown, with the stop signals corresponding to the crosslink sites denoted by large arrowheads (principal signals) or small arrowheads (weaker signals, or those not always seen). **A:** E- and P-site samples from lupin $tRNA^{Met}$ crosslinked to 16S RNA, using a primer for the primer extension reaction complementary to positions 779–795 of the 16S. **B:** P-site sample (lupin $tRNA^{Met}$ to 16S RNA), with primer complementary to positions 1412–1426. **C:** P-site sample (*E. coli* $tRNA^{Phe}$ crosslinked to 23S RNA), with primer complementary to positions 2212–2230. (The minor stop signal visible at position 2147 was only rarely observed.) **D:** P-site sample (lupin $tRNA^{Met}$ to 23S RNA), with primer complementary to positions 2639–2653.

A-site sample, and hence be now correctly assigned to the P site.

The interpretation of the data becomes somewhat more subtle in those cases where a particular crosslink is indeed formed from more than one of the three tRNA binding sites. Here, we exploit the fact that crosslinks are concomitantly formed from each tRNA-binding site to several positions on the ribosomal RNA. Suppose—again as an example—that crosslinks "x" and "y" are formed from the P site, and that crosslink "x" is also formed from the E site. If, in a particular experiment, the E-site complex was contaminated with a certain amount of P-site-bound tRNA, then we would expect to see both crosslinks "x" and "y" appearing as minor contaminating components in the E-site sample. If, on the other hand, we only observe crosslink "x" in the E-site sample, then we can interpret this as a genuine E-site crosslink. The crosslinks that are listed in Table 1 are based on reproducible observations of this nature from the ribonuclease H digestion data (cf. Fig. 1). The correctness of our interpretations is corroborated by the finding that, in some cases (Table 1, and see below), crosslinks from two or more tRNA binding sites to the same ribosomal RNA region (as evidenced by the ribonuclease H digestions) showed different stop signal patterns in the corresponding primer extension analyses (cf. Fig. 2), and thus do indeed represent distinct crosslink sites.

Crosslink sites on 23S rRNA

The most striking crosslink formed by TDB–$tRNA^{Met}$ was to the 900 region of the 23S RNA. This crosslink was entirely specific for the A site (Fig. 1A), and a combination of different ribonuclease H digestions served to localize the site to between nt 877 and 913 (Table 1). However, although the crosslink was reproducibly and strongly seen in the ribonuclease H experiments, no stop signal was found in the corresponding primer extension analyses. Similar examples of this phenomenon have been observed previously (Rinke-Appel et al., 1993; Stade et al., 1995), and most probably result from a crosslink to a ribose moiety or to some other position within a nucleotide that does necessarily cause the reverse transcriptase to pause or stop. A weak crosslink in the same region of the 23S RNA, also A-site specific, was found with APAB–$tRNA^{Phe}$ (Table 1), and here a faint primer extension signal was observed at position 890, suggesting a crosslink site at nt 889.

Weak crosslinking from all three sites was observed with TDB–$tRNA^{Met}$ between nt 1904 and 1933, whereas APAB–$tRNA^{Phe}$ showed a P-site-specific crosslink

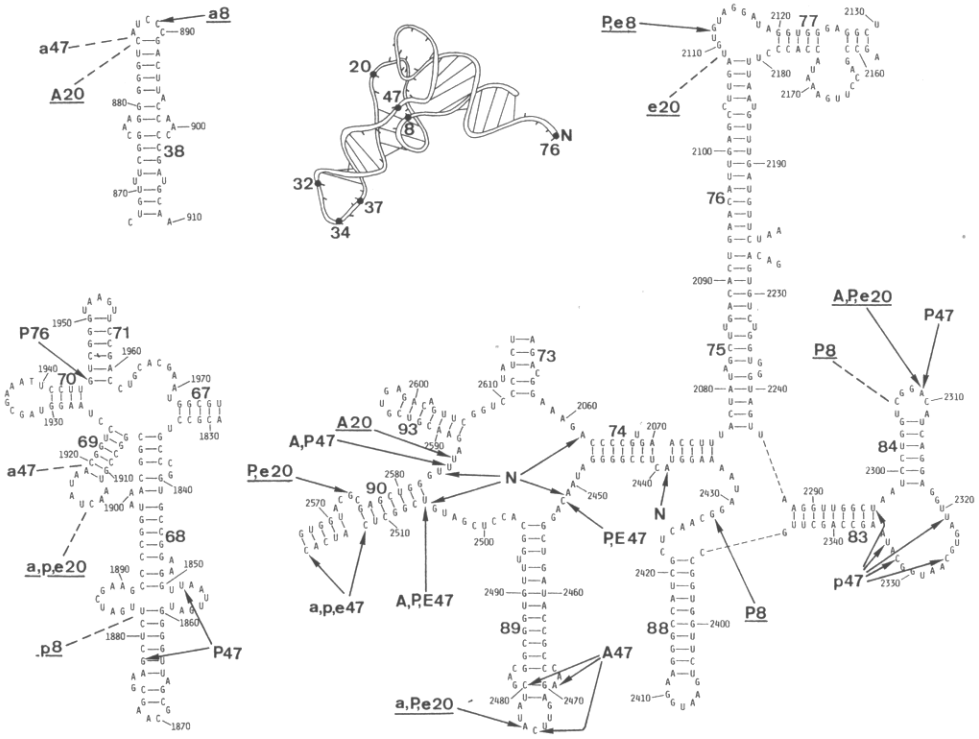

FIGURE 3. Locations of the crosslink sites (Table 1) in the corresponding regions of the secondary structure of 23S RNA, compared with other crosslinking data. The sketch of a tRNA molecule indicates the positions from which crosslinking data are available (see text for references); N denotes the aminoacyl residue. A-, P-, and E-site crosslinks are denoted by corresponding capital letters (major crosslinks) or small letters (minor crosslinks, or those not always seen), together with the tRNA position concerned (position 20:1 is for simplicity referred to as 20). Crosslinks indicated by dotted lines (as opposed to arrows) are those where no reverse transcriptase stop signal could be detected within the crosslinked region identified by ribonuclease H digestion (cf. Table 1). Data from this paper are underlined. Helices in the 23S RNA structure are numbered according to Leffers et al. (1987).

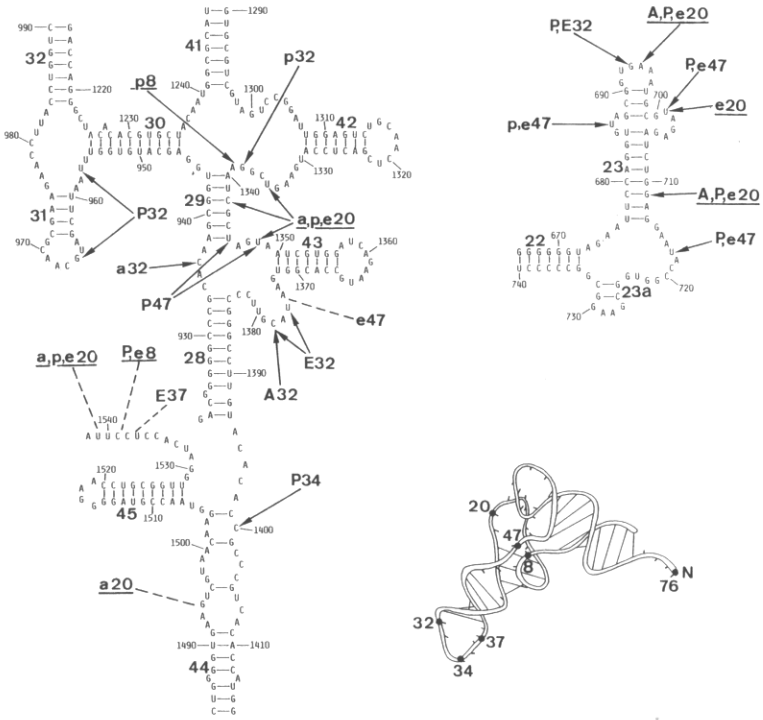

FIGURE 4. Locations of the crosslink sites (Table 1) in the corresponding regions of the secondary structure of 16S RNA, compared with other crosslinking data. The 16S RNA helices are numbered according to Brimacombe (1991). See legend to Figure 3 for further explanation.

nearby, between 1845 and 1892 (Table 1); here again no reverse transcriptase signals were found. TDB–tRNA^{Met} showed a minor E-site-specific site between 2088 and 2144 (cf. the somewhat longer fragment in the digest of Fig. 1B), and in the same area APAB–tRNA^{Phe} gave a major P-site crosslink (also observed more weakly from the E site, Fig. 1E), with primer extension stops indicative of crosslinks to nt 2111 and 2112 (Fig. 2C). In the 2300 region, TDB–tRNA^{Met} showed crosslinks from all three sites, most strongly from the A and P sites (Table 1), and the crosslink was localized to nt 2309 (Table 1; cf. Mitchell et al., 1993). In contrast, APAB–tRNA^{Phe} only showed weak P-site-specific crosslinking in this region (nt 2281–2358; Fig. 1F), and no primer extension signal was observed. With APAB–tRNA^{Phe} a P-site-specific crosslink was localized to the 2398–2442 region (with traces from the E site as well; cf. the corresponding longer fragment shown in Fig. 1G), and here the primer extension analyses indicated a crosslink site at nt 2428, although this stop signal was not seen in all experiments.

TDB–tRNA^{Met} showed crosslinking from all three sites (most prominently from the P site) to nt 2476 (Table 1), and a similar crosslinking pattern was found in the region between 2572 and 2603 (cf. the digest in Fig. 1C). In the latter case, the P-site crosslink (and also that from the E site) was localized to nt 2574 (Fig. 2D), whereas the A-site crosslink was localized to nt 2586 (Table 1), although in the latter case the stop signal was not always observed.

Crosslink sites on 16S rRNA

TDB–tRNA^{Met} gave crosslinking from all three sites to the 687–727 region of the 16S RNA (Table 1). The strong A- and P-site crosslinks were localized to nt 694 and 711 by primer extension analysis (see Fig. 2A for the P-site result), whereas the E-site crosslinking—although weaker in quantitative terms—reproducibly showed an additional site at nt 701 (Fig. 2A). Weaker and somewhat variable crosslinking was observed with TDB–tRNA^{Met} to the 3′ region of 16S RNA. This is typified by the example shown in Figure 1D, where crosslinking predominantly from the A and P sites to the 3′ 185 nt can be seen, together with crosslinking predominantly from the P and E sites between positions 1302 and 1358. In other experiments, the latter region also exhibited significant crosslinking from the A site (Table 1), and the crosslink sites were localized by primer extension analysis to nt 1342, with contributions from nt 1335 and 1348 (Fig. 2B). The crosslinking closer to the 3′ end was localized to the 3′-terminal 40 nt (Table 1), and a further weak A-site crosslink was sometimes observed between 1465 and 1500, although no primer extension signals were seen.

APAB–tRNA^{Phe} showed only low levels of crosslinking to the 16S RNA. No A-site-specific crosslink sites could be detected at all, whereas a weak P-site-specific crosslink was identified at nt 1338–1339. The most prominent crosslink was from the P site (and to a lesser extent from the E site) to the extreme 3′-terminus of the 16S RNA (nt 1531–1542, Table 1). The latter crosslink is illustrated in Figure 1H; on the left is a digest from the extreme 3′ terminus, whereas the digest on the right exemplifies a typical negative result, where no radioactive band is released corresponding to the excised fragment (the 30 nt between 1349 and 1378; digestion at the latter position is clearly incomplete) and the bands observed (195 and 165 nt) both arise from the extreme 3′-terminal crosslink.

DISCUSSION

Two distinct types of crosslinking approach have been applied to the study of contacts or neighborhoods between tRNA and rRNA. The first involves essentially "zero-length" crosslinking procedures, such as direct UV irradiation (Prince et al., 1982), or the use of azido derivatives incorporated into a purine base in the tRNA (e.g., Wower et al., 1989). This approach gives very precise information, but has the concomitant disadvantage that from many positions of the tRNA there may not be a potential crosslinking target on the rRNA that is sufficiently close to react. The alternative approach, which has been used frequently to study neighborhoods between tRNA and ribosomal proteins (e.g., Ofengand et al., 1986) and which we have exploited here, makes use of natural modifications in the tRNA in order to attach a photoreactive ligand. The reagents usually employed—as in the experiments here—have a fully extended length of ca. 7–8 Å, which, in the case of acp^{3}U, effectively becomes 10–11 Å due to the length of the side chain on the acp^{3}U residue to which the reagent is attached (Podkowinski & Gornicki, 1991). With this method, sites on the rRNA can be crosslinked from many more positions on the tRNA, but the information obtained is correspondingly less precise; the same site on the rRNA can, in principle, be reached from positions on the tRNA that are up to ca. 20 Å apart, or similarly from tRNAs that are bound to different ribosomal sites. This property is reflected in the overall patterns of crosslinking data, which are summarized in Figure 3 for the 23S RNA and in Figure 4 for the 16S RNA.

The data sets illustrated in Figures 3 and 4 include the direct UV crosslink from position 34 of P-site-bound tRNA (Prince et al., 1982), and the crosslinks from azidonucleotides at positions 37 (Wower et al., 1993) and 76 (Wower et al., 1989), as well as our own data from positions 32 (Döring et al., 1994), 47 (Mitchell et al., 1993; Osswald et al., 1995), and 8 and 20:1 (this paper). In addition, crosslinks are included that have been observed from a derivatized aminoacyl residue attached to the 3′ terminus of the tRNA (Steiner et al.,

1988; Mitchell et al., 1993; Stade et al., 1994). The overall pattern is—as expected—that, whereas crosslinks from the anticodon loop region are exclusively to the 16S RNA and those from the CCA end or aminoacyl residue are exclusively to the 23S RNA, crosslinks from the central fold region are to both rRNA molecules.

Environment of tRNA on 23S rRNA

The crosslinking data for 23S RNA (Fig. 3) are grouped within five distinct regions of the molecule. The most unexpected result is the observation of A-site-specific crosslinking from all three positions (8, 47, and 20:1) of the central fold of the tRNA to helix 38 (Fig. 3, upper left). Although in the most prominent case (from position 20:1, Fig. 1A) the crosslink site could not be pin-pointed by primer extension, the ribonuclease H data (Table 1) clearly localize the crosslink to a ca. 35-nt region at the loop-end of this long helix (only about one-third of the helix is shown in Fig. 4). Helix 38 has not so far been implicated as being close to a functional area of the ribosomal RNA, and its location within the 3D structure of the 23S RNA is not constrained by other topographical data (cf. Brimacombe, 1995).

Several crosslinks—the second group—occur within helices 68–70 in Domain IV of the 23S RNA (Fig. 3, lower left), including the crosslink to base 1945 from an azidonucleotide at position 76 of the tRNA (Wower et al., 1989). This area of the 23S RNA has been shown by direct UV crosslinking to lie close to the peptidyl transferase center (Brimacombe, 1995), and moreover, helix 69 has been crosslinked to 16S RNA (Mitchell et al., 1992), and therefore probably forms part of the interface bridge (Frank et al., 1995; Stark et al., 1995) connecting the 30S and 50S subunits. On the other hand, helix 68, which exhibits crosslink sites from positions 47 and 8 of P-site tRNA, also has a crosslink site to protein L1 (Brimacombe, 1991). This helix is accordingly already topographically "linked" to the third group of tRNA crosslink sites, namely those between helices 76 and 77 (Fig. 3, upper right), where the binding site for protein L1 (Branlant et al., 1976) is located, as well as further crosslink sites to this protein (Brimacombe, 1991). The corresponding well-defined P-site crosslinks at nt 1852 and 1878 from position 47 of the tRNA, and at nt 2111–2112 from position 8 (Figs. 1E, 2C) thus suggest that the central fold of the P-site tRNA is close to the L1 protuberance of the 50S subunit. Furthermore, nt 2112 has been identified as a CCA-end dependent E-site footprint position (Moazed & Noller, 1989a); because the E-site tRNA (having released its peptidyl moiety) is no longer constrained to the peptidyl transferase center at its CCA end, the crosslink site from position 8 of P-site tRNA to the same nucleotide helps to define the relative orientations of the P- and E-site tRNAs in this area of the 23S molecule. E-site-specific crosslinking from position 20:1 was also observed in this region (Table 1).

The fourth group of crosslink sites is in the region of helices 83 and 84 (Fig. 3, lower right). By virtue of crosslinks to proteins L5, L18, and L27 (Brimacombe, 1991), this part of the 23S RNA belongs to the vicinity of the central protuberance of the 50S subunit (cf. Walleczek et al., 1988). The crosslinks here are largely from the P site, nt 2309 being the most prominent target of crosslinking (cf. Mitchell et al., 1993). Nucleotide 2309 is also crosslinked from position 20:1 of A-site tRNA. If the A- and P-site tRNAs are arranged in the "S" configuration (Lim et al., 1992; Easterwood et al., 1994), then the D-loop of the A-site tRNA faces the P site. The S configuration is the one that we now favor in our model-building studies (Stark et al., 1995), and therefore an "overlap" between A-site crosslinking from position 20:1 and P-site crosslinking from positions 8 or 47 is not unreasonable.

The latter argument cannot, however, be used to explain the large number of A-, P-, and E-site crosslinks from positions 20:1 and 47 in the fifth and final group of sites on the 23S RNA, namely those at the peptidyl transferase center (Fig. 3, lower middle), which is the ring enclosed by helices 73, 74, 89, 90, and 93 (Vester & Garrett, 1988). Here, there is a much greater "overlap" in the crosslinking data, the most extreme example being nt 2505, which is crosslinked to the aminoacyl residue of P- and A-site tRNA (Steiner et al., 1988; Stade et al., 1994) and is also crosslinked from position 47 of tRNA at all three sites, as well as being footprinted by P-site tRNA (Moazed & Noller, 1989a). The distance between position 47 and an aminoacyl residue attached to position 76 (ca. 50 Å) is too large to be bridged by the lengths of the respective crosslinking reagents (ca. 10 Å), and concomitant crosslinking to the same nucleotide on the rRNA therefore implies either a flexibility of the tRNA-binding sites or a flexibility in the structures of the tRNA and rRNA molecules themselves. The crosslinking to the loop-end of helix 89 is interesting in this respect, because this loop-end has also been crosslinked to loop IV of 5S RNA (Dontsova et al., 1994). Dohme and Nierhaus (1976) have reported that 50S subunits lacking 5S RNA show a greatly reduced level of EF-Tu-dependent A-site tRNA binding, and the crosslinking from position 47 of A-site tRNA to helix 89 is compatible with this observation. Helix 89, furthermore, contains a strong crosslink site to protein L6 (Brimacombe, 1991), which is located on the L7/12 stalk side of the central protuberance of the 50S subunit (Walleczek et al., 1988), close to where A-site binding would be expected (Stark et al., 1995). On the other hand, the same loop-end of helix 89 is crosslinked from position 20:1 of P-site tRNA, and Muralikrishna and Cooperman (1995) have crosslinked this area (albeit using a rather long reagent) to protein L1, on the other side of the central protuberance. Taken together, these

results are incompatible with one another and suggest that helix 89 may be involved in quite large conformational changes within the ribosome. "Hybrid" or intermediate tRNA-binding sites (Moazed & Noller, 1989b) may also contribute to the complexity of the crosslinking patterns here.

It is noteworthy that there are no crosslinks from position 8 of the tRNA to the peptidyl transferase area, with the exception of the P-site crosslink tentatively located to nt 2428 (not far from the E-site footprint at nt 2394 [Moazed & Noller, 1989a]). This lack of reactivity may merely be due to our use of an azido reagent to modify position 8, the azido compounds being in general not as reactive as the corresponding diazirines (Bochkariov & Kogon, 1992).

Environment of tRNA on 16S rRNA

The corresponding crosslinking data for 16S RNA (Fig. 4) are grouped into three regions of the molecule, the first of which is helix 23 (Fig. 4, upper right). The crosslinks here are predominantly from positions 20:1, 32, and 47 of P- and E-site tRNA, and one of them is notably an E-site-specific crosslink at nt 701 (Fig. 2A) from position 20:1. Significant crosslinking from position 20:1 of A-site tRNA was, however, also seen, and—as with the crosslinks to the peptidyl transferase region (above)—this concomitant crosslinking to the same nucleotides in the helix 23 area from all three tRNA sites is difficult to explain without invoking some flexibility of the tRNA or rRNA structures. Current model-building studies (Brimacombe, 1995; Stark et al., 1995) place helix 23 on the side lobe of the 30S subunit; Ofverstedt et al. (1994) have demonstrated that "starved" ribosomes have a more open configuration than actively functioning ones, and the side lobe of the 30S subunit is a likely candidate to be involved in the change between these states.

Nucleotide 693 in helix 23 is a footprint site for P-site tRNA (Moazed & Noller, 1990), and several crosslink and footprint sites coincide with each other in the second 16S RNA region, namely helices 28–31 (Fig. 4, left). Notably, two of the footprint positions concerned, nt 966 and 1338, are among those that have been found to be essential for P-site tRNA binding, although 1338 was only observed in some experiments (von Ahsen & Noller, 1995). A "chain" of P-site crosslinks between nt 1338 and 1348 can be seen in this part of the 16S RNA, from positions 8, 20:1, 32, and 47 of the tRNA. Helices 28–43 form the "head" of the 30S subunit and, in our current model for the 16S RNA (cf. Brimacombe, 1995), helix 29—which encompasses this chain of crosslinks—is placed "under the chin" of the 30S subunit head. Also noteworthy here are the A- and E-site crosslinks from position 32 of tRNA already reported (Döring et al., 1994) in the loop connecting helices 28 and 43, with an E-site crosslink from position 47 occurring in the same sequence region.

Curiously, we have not observed any significant crosslinking of tRNA to the 1400 region of the 16S RNA, where the "classical" P-site crosslink from position 34 (Prince et al., 1982) is located, and that is believed to represent the primary decoding region (e.g., Purohit & Stern, 1994); possibly the tRNA–mRNA–16S RNA contacts are too closely packed in this area to allow a bulky aromatic crosslinking reagent to penetrate into the functional complex. Crosslinking was, however, observed to the extreme 3′-terminal section of the 16S RNA (the third group of sites) in several cases (cf. Wower et al., 1993).

Taken together, the crosslinks illustrated in Figures 3 and 4 offer an intricate pattern of data, which will be of considerable help—and at the same time a challenge—in the continuing process of deducing the 3D structure and dynamics of the functional regions of the 16S and 23S ribosomal RNA molecules. As noted in the Introduction, our future model-building studies (cf. Stark et al., 1995) will have to take these data into account.

MATERIALS AND METHODS

Derivatization and charging of tRNAs

Lupin elongator $tRNA^{Met}$ was a generous gift from Dr. P. Gornicki (Poznan). *E. coli* $tRNA^{Phe}$ was obtained from Boehringer, Mannheim, or Biogenes, Berlin. In both cases, the tRNA was dephosphorylated and labeled with ^{32}P at its 5′ end, by the procedure of Gnirke et al. (1989); the $tRNA^{Phe}$ was purified by electrophoresis on a 15% polyacrylamide gel prior to labeling. Specific activities of the ^{32}P-labeled tRNAs were of the order of 40,000 cpm/pmol. Derivatization with TDB (Bochkareva et al., 1988; kindly provided by D. Bochkariov) or APAB (Hixson & Hixson, 1975) was carried out in DMSO under the conditions of Bochkariov and Kogon (1992). Excess reagent was removed by passing the reaction mixture over a NAP column (Pharmacia) in the case of TDB modification, or by several ethanol precipitations in the case of APAB. The uncharged derivatized tRNAs were used for binding to the ribosomal P or E sites. For A-site binding, the derivatized TDB–$tRNA^{Met}$ was charged with methionine by the method of Rheinberger et al. (1988) using S100 prepared from lupin seeds (a generous gift from Dr. T. Twardowski, Poznan); the charged TDB–$tRNA^{Met}$ was purified on a NAP column, the level of charging being 20–25%, as determined in parallel experiments using 14C-labeled methionine and unlabeled TDB–$tRNA^{Met}$. (Under the same conditions, nonderivatized $tRNA^{Met}$ was charged to 25–30%). In the case of $tRNA^{Phe}$, charging was carried out prior to APAB modification, the corresponding charging level being ca. 70%.

Binding of derivatized tRNAs to the ribosomal A, P, and E sites

mRNA analogues were prepared by T7 transcription from synthetic DNA templates (custom synthesized by TIB, Ber-

lin) by our usual procedure (Stade et al., 1989; Dontsova et al., 1992). For binding of charged or uncharged TDB–$tRNA^{Met}$ to all three ribosomal sites, an mRNA ("mRNA-1") was used with the sequence GGGAGAAAAGA **CGU AUG GAA** AAAAACAAAAACAAAAC, whereby the codons in bold type are for Arg, Met, and Glu, respectively. For A- and P-site binding of APAB–$tRNA^{Phe}$ (charged or uncharged, respectively), "mRNA-2" was used, with the sequence GGGA GAGGAGAAAAGAAG **AUG UUC** AAAAGAAAA, the codons in bold type being for Met and Phe. For E-site binding of APAB–$tRNA^{Phe}$, "mRNA-3" was used, which was the same as mRNA-2, but with the **AUG UUC** sequence changed to **UUC AUG**. For tRNA binding, reaction mixtures were prepared containing 250 pmol of 70S tight couple ribosomes from *E. coli* MRE 600, or ribosomes reconstituted from 30S and 50S subunits, in both cases as described by Döring et al. (1994), except that with the lupin TDB–$tRNA^{Met}$, magnesium concentrations of 10 mM and 15 mM were used in place of 7.5 mM and 10 mM, respectively.

Binding of charged TDB–$tRNA^{Met}$ to the A site was made in the presence of EF-Tu, with mRNA-1 and $tRNA_I^{Arg}$ (Subriden RNA, USA) at the P site. A-site binding of APAB–$tRNA^{Phe}$ was carried out similarly, using mRNA-2 and $tRNA^{fMet}$ (Boehringer, Mannheim). P-site binding of uncharged TDB–$tRNA^{Met}$ or APAB–$tRNA^{Phe}$ was made directly, with mRNA-1 or mRNA-2, respectively. For E-site binding of APAB–$tRNA^{Phe}$, mRNA-3 was used together with $tRNA^{fMet}$ at the P site, as described by Döring et al. (1994). E-site binding of TDB–$tRNA^{Met}$ was made either with mRNA-1 in the presence of $tRNA^{Glu}$ (Subriden RNA, USA) at the P site, again as described by Döring et al. (1994), or with mRNA-1 and Glu–$tRNA^{Glu}$ at the A site, followed by treatment with EF-G to translocate the TDB–$tRNA^{Met}$ from the P to the E site, using the procedure of Rinke-Appel et al. (1993).

Isolation and analysis of crosslinked products

Ribosomal complexes containing TDB–$tRNA^{Met}$ were irradiated in the cold for 10 min at 350 nm, as described by Tate et al. (1990). Complexes containing APAB–$tRNA^{Phe}$ were also irradiated for 10 min in the cold, but in this case using a UV lamp with an energy maximum at 254 nm, the samples being covered by a glass plate with a 280-nm cut-off as described by Stade et al. (1989). In all cases, the irradiated samples were applied to sucrose gradients as in Stade et al. (1989) so as to isolate ribosomal proteins or rRNA crosslinked to the derivatized $tRNA^{Met}$ or $tRNA^{Phe}$. Crosslinked proteins were identified immunologically (Gulle et al., 1988). Crosslink sites on the rRNA were localized by treatment with ribonuclease H in the presence of selected pairs of oligodeoxynucleotides (Dontsova et al., 1992; Döring et al., 1994), followed by primer extension analysis (Moazed et al., 1986; Döring et al., 1994), according to our usual procedures.

ACKNOWLEDGMENTS

We are most grateful to Dr. Dmitry Bochkariov for providing us with the diazirine reagent, Dr. Piotr Gornicki for the lupin $tRNA^{Met}$, and Dr. Tomasz Twardowski for the S100 supernatant from lupin seeds. The work was supported in part by a grant from the Deutsche Forschungsgemeinschaft (Br 632/3-2).

Received September 14, 1995; returned for revision November 3, 1995; revised manuscript received November 17, 1995

REFERENCES

Abdurashidova GG, Tsvetkova EA, Budowsky EI. 1989. Nucleotide residues of tRNA, directly interacting with proteins within the complex of the 30S subunit of *E. coli* ribosome with poly(U) and NAcPhe–$tRNA^{Phe}$. *FEBS Lett 243*:299–302.

Abdurashidova GG, Tsvetkova EA, Budowsky EI. 1990. Determination of tRNA nucleotide residues directly interacting with proteins in the post- and pretranslocated ribosomal complexes. *FEBS Lett 269*:398–401.

Bochkareva ES, Lissin NM, Girshovich AS. 1988. Transient association of newly synthesized unfolded proteins with the heat-shock GRoEL protein. *Nature 336*:254–257.

Bochkariov DE, Kogon AA. 1992. Application of 3-[3-(3-trifluoromethyldiazirin-3-yl)phenyl]-2,3-dihydroxypropionic acid, carbene generating, cleavable crosslinking reagent for photoaffinity labeling. *Anal Biochem 204*:90–95.

Branlant C, Korobko V, Ebel JP. 1976. The binding site of protein L1 on 23S ribosomal RNA from *E. coli*. *Eur J Biochem 70*:471–482.

Brimacombe R. 1991. RNA–protein interactions in the *E. coli* ribosome. *Biochimie 73*:927–936.

Brimacombe R. 1995. The structure of ribosomal RNA; a three-dimensional jigsaw puzzle. *Eur J Biochem 230*:365–383.

Brunner J, Senn H, Richards FM. 1980. 3-Trifluoromethyl-3-phenyldiazirine. A new carbene generating group for photolabeling reagents. *J Biol Chem 255*:3313–3318.

Dohme F, Nierhaus KH. 1976. Role of 5S RNA in assembly and function of the 50S subunit from *E. coli*. *Proc Natl Acad Sci USA 73*: 2221–2225.

Dontsova O, Dokudovskaya S, Kopylov A, Bogdanov AA, Rinke-Appel J, Jünke N, Brimacombe R. 1992. Three widely separated positions in 16S RNA lie in or close to the ribosomal decoding region; a site-directed cross-linking study with mRNA analogues. *EMBO J 11*:3105–3116.

Dontsova O, Tishkov V, Dokudovskaya S, Bogdanov A, Döring T, Rinke-Appel J, Thamm S, Greuer B, Brimacombe R. 1994. Stem-loop IV of 5S rRNA lies close to the peptidyl transferase center. *Proc Natl Acad Sci USA 91*:4125–4129.

Döring T, Mitchell P, Osswald M, Bochkariov D, Brimacombe R. 1994. The decoding region of 16S RNA; a cross-linking study of the ribosomal A, P and E sites using tRNA derivatized at position 32 in the anticodon loop. *EMBO J 13*:2677–2685.

Easterwood TR, Major F, Malhotra A, Harvey SC. 1994. Orientations of transfer RNA in the ribosomal A and P sites. *Nucleic Acids Res 22*:3779–3786.

Frank J, Penczek P, Grassucci R, Srivastava S. 1991. Three-dimensional reconstruction of the 70S *E. coli* ribosome in ice: The distribution of ribosomal RNA. *J Cell Biol 115*:597–605

Frank J, Zhu J, Penczek P, Li Y, Srivastava S, Verschoor A, Radermacher M, Grassucci R, Lata RK, Agrawal RK. 1995. A model of protein synthesis based on cryo-electron microscopy of the *E. coli* ribosome. *Nature 376*:441–444.

Gnirke A, Geigenmüller U, Rheinberger HJ, Nierhaus KH. 1989. The allosteric three-site model for the ribosomal elongation cycle. Analysis with a heteropolymeric mRNA. *J Biol Chem 264*:7291–7301.

Gulle H, Hoppe E, Osswald M, Greuer B, Brimacombe R, Stöffler G. 1988. RNA–protein cross-linking in *E. coli* 50S ribosomal subunits; determination of sites on 23S RNA that are cross-linked to proteins L2, L4, L24 and L27 by treatment with 2-iminothiolane. *Nucleic Acids Res 16*:815–832.

Hixson SH, Hixson SS. 1975. *p*-Azidophenacyl bromide, a versatile photolabile bifunctional reagent. Reaction with glyceraldehyde-3-phosphate dehydrogenase. *Biochemistry 14*:4251–4254.

Hsu LM, Lin FL, Nurse K, Ofengand J. 1984. Covalent cross-linking of *E. coli* phenylalanyl-tRNA and valyl-tRNA to the ribosomal A

site via photoaffinity probes attached to the 4-thiouridine residue. *J Mol Biol 172*:57–76.

Leffers H, Kjems J, Ostergaard L, Larsen N, Garrett RA. 1987. Evolutionary relationships amongst archaebacteria. A comparative study of 23S ribosomal RNAs of a sulphur-dependent extreme thermophile, an extreme halophile and a thermophilic methanogen. *J Mol Biol 195*:43–61.

Lim V, Venclovas C, Spirin A, Brimacombe R, Mitchell P, Mueller F. 1992. How are tRNAs and mRNA arranged in the ribosome? An attempt to correlate the stereochemistry of the tRNA–mRNA interaction with constraints imposed by the ribosomal topography. *Nucleic Acids Res 20*:2627–2637.

Lin FL, Kahan L, Ofengand J. 1984. Cross-linking of phenylalanyl-tRNA to the ribosomal A site via a photoaffinity probe attached to the 4-thiouridine residue is exclusively to ribosomal protein S19. *J Mol Biol 172*:77–86.

Mitchell P, Osswald M, Brimacombe R. 1992. Identification of intermolecular RNA cross-links at the subunit interface of the *E. coli* ribosome. *Biochemistry 31*:3004–3011.

Mitchell P, Stade K, Osswald M, Brimacombe R. 1993. Site-directed cross-linking studies on the *E. coli* tRNA-ribosome complex: Determination of sites labelled with an aromatic azide attached to the variable loop or aminoacyl group of tRNA. *Nucleic Acids Res 21*:887–896.

Moazed D, Noller HF. 1989a. Interaction of tRNA with 23S rRNA in the ribosomal A, P and E sites. *Cell 57*:585–597.

Moazed D, Noller HF. 1989b. Intermediate states in the movement of tRNA in the ribosome. *Nature 342*:142–148.

Moazed D, Noller HF. 1990. Binding of tRNA to the ribosomal A and P sites protects two distinct sets of nucleotides in 16S rRNA. *J Mol Biol 211*:135–145.

Moazed D, Stern S, Noller HF. 1986. Rapid chemical probing of conformation in 16S ribosomal RNA and 30S ribosomal subunits using primer extension. *J Mol Biol 187*:399–416.

Muralikrishna P, Cooperman BS. 1995. Ribosomal components neighboring the 2475 loop in *E. coli* 50S subunits. *Biochemistry 34*:115–121.

Ofengand J, Ciesiolka J, Denman R, Nurse K. 1986. Structural and functional interactions of the tRNA-ribosome complex. In: Hardesty B, Kramer G, eds. *Structure, function and genetics of ribosomes*. New York: Springer-Verlag. pp 473–494.

Ofverstedt LG, Zhang K, Tapio S, Skogland U, Isaksson LA. 1994. Starvation in vivo for aminoacyl-tRNA increases the spatial separation between the two ribosomal subunits. *Cell 79*:629–638.

Osswald M, Döring T, Brimacombe R. 1995. The ribosomal neighbourhood of the central fold of tRNA; cross-links from position 47 of tRNA located at the A, P or E site. *Nucleic Acids Res 23*: 4635–4641.

Podkowinski J, Gornicki P. 1991. Neighbourhood of the central fold of the tRNA molecule bound to the *E. coli* ribosome—Affinity labeling studies with modified tRNAs carrying photoreactive probes attached to the dihydrouridine loop. *Nucleic Acids Res 19*:801–808.

Prince JB, Taylor BH, Thurlow DL, Ofengand J, Zimmermann RA. 1982. Covalent cross-linking of $tRNA_1^{Val}$ to 16S RNA at the ribosomal P site: Identification of cross-linked residues. *Proc Natl Acad Sci USA 79*:5450–5454.

Purohit P, Stern S. 1994. Interactions of a small RNA with antibiotic and RNA ligands of the 30S subunit. *Nature 370*:659–662.

Rheinberger HJ, Geigenmüller U, Wedde M, Nierhaus KH. 1988. Parameters for the preparation of *E. coli* ribosomes and ribosomal subunits active in tRNA binding. *Methods Enzymol 164*:658–670.

Rinke-Appel J, Jünke N, Brimacombe R, Dokudovskaya S, Dontsova O, Bogdanov A. 1993. Site-directed cross-linking of mRNA analogues to 16S ribosomal RNA; a complete scan of cross-links from all positions between +1 and +16 on the mRNA, downstream from the decoding site. *Nucleic Acids Res 21*:2853–2859.

Smith D, Yarus M. 1989. tRNA–tRNA interactions within cellular ribosomes. *Proc Natl Acad Sci USA 86*:4397–4401.

Stade K, Jünke N, Brimacombe R. 1995. Mapping the path of the nascent peptide chain through the 23S RNA in the 50S ribosomal subunit. *Nucleic Acids Res 23*:2371–2380.

Stade K, Riens S, Bochkariov D, Brimacombe R. 1994. Contacts between the growing peptide chain and the 23S RNA in the 50S ribosomal subunit. *Nucleic Acids Res 22*:1394–1399.

Stade K, Rinke-Appel J, Brimacombe R. 1989. Site-directed cross-linking of mRNA analogues to the *E. coli* ribosome; identification of 30S ribosomal components that can be cross-linked to the mRNA at various points 5′ with respect to the decoding site. *Nucleic Acids Res 17*:9889–9908.

Stark H, Mueller F, Orlova EV, Schatz M, Dube P, Erdemir T, Zemlin F, Brimacombe R, van Heel M. 1995. The 70S *E. coli* ribosome at 23 Å resolution: Fitting the ribosomal RNA. *Structure 3*:815–821.

Steiner G, Kuechler E, Barta A. 1988. Photo-affinity labelling at the peptidyl transferase centre reveals two different positions for the A- and P-sites in domain V of 23S rRNA. *EMBO J 7*:3949–3955.

Sundaralingam M, Brennan T, Yathindra N, Ichikawa T. 1975. Stereochemistry of mRNA (codon)–tRNA(anticodon) interaction on the ribosome during peptide bond formation. In: Sundaralingam M, Rao ST, eds. *Structure and conformation of nucleic acids and protein-nucleic acid interactions*. Baltimore, Maryland: University Park Press. pp 101–115.

Tate W, Greuer B, Brimacombe R. 1990. Codon recognition in polypeptide chain termination: Site-directed cross-linking of termination codon to *E. coli* release factor 2. *Nucleic Acids Res 18*:6537–6544.

Vester B, Garrett RA. 1988. The importance of highly conserved nucleotides in the binding region of chloramphenicol at the peptidyl transferase centre of *E. coli* ribosomal RNA. *EMBO J 7*:3577–3587.

von Ahsen U, Noller HF. 1995. Identification of bases in 16S rRNA essential for tRNA binding at the 30S ribosomal P site. *Science 267*:234–237.

Walleczek J, Schüler D, Stöffler-Meilicke M, Brimacombe R, Stöffler G. 1988. A model for the spatial arrangement of the proteins in the large subunit of the *E. coli* ribosome. *EMBO J 7*:3571–3576.

Wower J, Hixson SS, Zimmermann RA. 1989. Labeling the peptidyl transferase center of the *E. coli* ribosome with photoreactive $tRNA^{Phe}$ derivatives containing azidoadenosine at the 3′ end of the acceptor arm; a new model of the tRNA–ribosome complex. *Proc Natl Acad Sci USA 86*:5232–5236.

Wower J, Scheffer P, Sylvers LA, Wintermeyer W, Zimmermann RA. 1993. Topography of the E site on the *E. coli* ribosome. *EMBO J 12*:617–623.

The ribosomal environment of tRNA: crosslinks to rRNA from positions 8 and 20:1 in the central fold of tRNA located at the A, P, or E site.

J Rinke-Appel, N Jünke, M Osswald, et al.

RNA 1995 1: 1018-1028